THE N-SHAPED CURRENT-POTENTIAL CHARACTERISTIC IN FROG SKIN

I. Time Development during Step Voltage Clamp

HARVEY M. FISHMAN *and* ROBERT I. MACEY

From the Department of Physiology-Anatomy, University of California, Berkeley, California 94720. Dr. Fishman's present address is the Laboratory of Biophysics, National Institute of Neurological Diseases and Stroke (NINDS)-National Institutes of Health, Bethesda, Maryland 20014.

ABSTRACT A fast (10 μsec) voltage-clamp system similar to that used on nerve axons was applied across the frog skin. An electrical analog is used to obtain the electrical parameters and to estimate the time (300 μsec) required to voltage clamp the excitable membrane layer in the skin. The speed of the clamp allows observation of the early development in time of an N-shaped current-potential (I-V) relation. The isochronal I-V curves constructed from step clamp data show the beginning of a negative slope in about 250 μsec after successively applied step changes in skin potential (> 200 mv). Subsequently, the negative slope reaches a quasi-steady state interval (0.4–1.5 msec) and then decays and disappears in the next 20 msec. The negative slope I-V characteristic is only found in skins which exhibit spike generation under current clamp.

INTRODUCTION

Electrical excitability in frog skin was discovered by Finkelstein (1961, 1964). In a subsequent study, Lindemann (1965) indicated that a current-potential (I-V) relation constructed from step-voltage clamp data had a characteristic N-shape, which seems to be common to all excitable membranes. This paper describes step voltage-clamp experiments which measure the kinetic development of the I-V relation. A separation of the ionic current from the early capacitive transient shortly after an above-threshold step change in skin potential shows the onset of a negative-resistance process in the skin in about 100 μsec. The negative slope I-V characteristic is found if and only if the skin is capable of spike generation under current clamp.

Because of the many cell layers in frog skin, it has often been difficult to relate macroscopic measurements to specific structures in the skin. This situation is somewhat improved by recent evidence localizing spike generation to the outermost cell membranes of the epidermis by micropuncture study (Lindemann and Thorns, 1967) and by a "split" skin preparation in which the calcium-dependent excitable

process was found to occur at this surface (Fishman and Macey, 1968). Nevertheless, spike generation is detected across either the entire skin or the isolated epidermis and it is these preparations which have been voltage clamped.

MATERIALS AND METHODS

Skin Preparation

The abdominal skin from grass frogs[1] (usually *Rana pipiens*) of both sexes was used. After removal from the animal, the skin was placed in Ringer's solution (115 mM NaCl, 5 mM KCl, 2 mM $CaCl_2$, 8 mM Tris and 2 g/liter glucose pH = 8.0) for 10–15 min. A "split" skin preparation (the epidermis with the dermis removed) as described by Fishman and Macey (1968) was also used. The skin was placed between two Lucite chambers with 1 cm^2

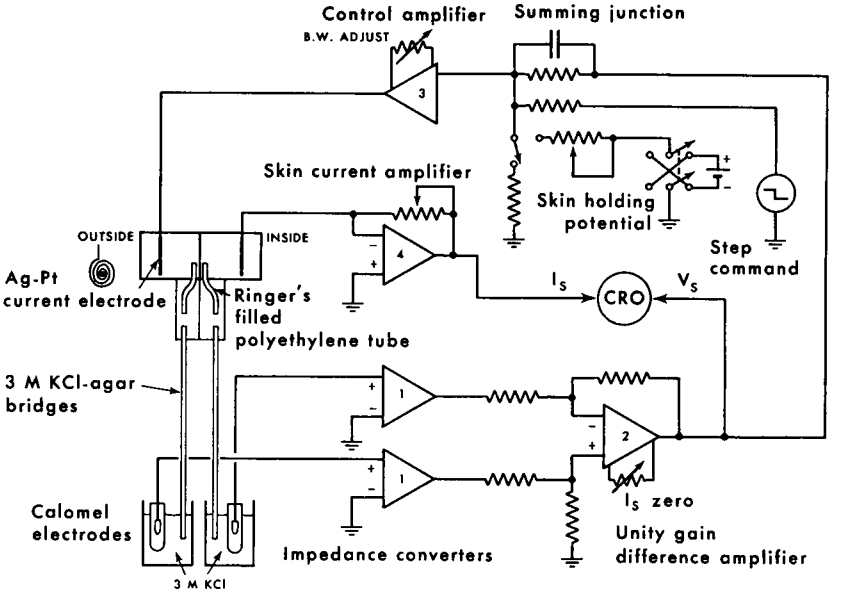

FIGURE 1 Schematic diagram of the measurement and control system. See text for description.

disk of skin exposed to Ringer's solution on both sides. The solution in contact with the inside surface of the skin was bubbled with air. The potential difference across the skin (Fig. 1) was obtained from two calomel electrodes which communicated through 3 M KCl-agar bridges with Ringer's-filled polyethylene tubes placed parallel to and against the inside and ouside surfaces of the skin. The tubes did not block the current path to the skin in the region of the skin where the potential was being monitored. Two platinized-silver (planar spiral) electrodes (Cole and Kishimoto, 1962) were placed about 2 cm from the surface of the skin on each side and used to pass current through the solutions and the skin.

[1] Experiments were not confined to a particular species of grass frog since the excitable property was found in many different species.

Current Clamp

Rectangular pulses of current were passed through the skin from a Tektronix type 161 pulse generator (Tektronix, Inc., Beaverton, Ore.) in series with 100 kΩ. The skin potential responses were recorded using the skin potential sensing portion of the voltage-clamp system described below.

Voltage Clamp

A schematic diagram of the complete voltage-clamp system is shown in Fig. 1. The potential developed at the calomel electrodes (80 kΩ resistance) was passed through two identical impedance converters (unity gain, field effect-transistor input amplifiers—# 1) which presented a high input resistance ($10^{11}\Omega$) to the calomel electrodes and a low output impedance to a difference operational amplifier (# 2, a Zeltex (Zeltex, Inc., Concord, Calif.) 132) also of unity gain. The potential difference across the skin obtained from the difference amplifier (# 2) output was observed on a cathode-ray oscilloscope and also compared at the summing junction (input) of the control amplifier (# 3) with a DC holding potential[2] and a step command pulse from the Tektronix type 161 pulse generator. The output of the control amplifier (# 3, a Zeltex 147) supplied a current through the skin so that the difference between the sum of the holding and command potentials as compared to the skin potential was negligible ($<0.1\%$). The current through the skin was detected by an operational amplifier (# 4, a Burr Brown 1506, Burr-Brown Research Corp., Tucson, Ariz.). The input to the operational amplifier was connected to the inside platinized-silver electrode providing a virtual ground at this point. The current through the skin was collected at this current electrode and provided an input to the amplifier (# 4). The voltage output of the amplifier (# 4) was thus proportional to this current. The skin potential and current were recorded on a Tektronix type 564 storage oscilloscope.

Stability Considerations

There are three essential stability requirements in a voltage-clamp system. The first concerns the closed-loop stability of the measurement system. The degree of system stability can be determined from the amount of overshoot in the step response of the system closed around a substitute preparation (a lumped electrical model of the resting frog skin). As in other voltage-clamp systems, a lead (high frequency accentuation) network was placed in the loop (at the summing junction in Fig. 1) and the bandwidth of the control amplifier (# 3) adjusted so that the closed-loop step response gave an overshoot $\leq 5\%$ (5% overshoot gives minimum response time and adequate stability, [Cole, 1968, 83]). The rise time (time to clamp the voltage across the entire skin) of the system in Fig. 1 was measured to be 10 μsec with a skin in the chamber. Most of the rise time limitation resulted from the reduction in loop bandwidth associated with the stray capacity to ground in the paths from the skin surfaces to the impedance converters.

The second stability criterion concerns system control of the active property of the preparation. (Cole and Moore, 1960, Appendix D). The clamp system output impedance (including the current electrode resistances and solution resistances up to the potential sensing

[2] In the experiments described in this paper the holding potential was zero volts. Thus, in the quiescent voltage-clamp state the current through the skin was the short-circuit current, which has been shown to be a measure of Na pump activity (Ussing and Zerahn, 1951).

electrodes) must be smaller than the absolute magnitude of the lowest negative resistance which the excitable preparation attains when it becomes active. The "quasi-steady state" negative resistance obtained from voltage-clamp measurements is used as an approximation for the actual negative resistance in the preparation. The lowest value found in frog skin in these experiments was $-150\ \Omega \cdot cm^2$. The output impedance of the system in Fig. 1 was measured by introducing a constant current at the outside current electrode and measuring the resulting perturbation in skin potential. The system output impedance measured in this manner was $< 3\ \Omega \cdot cm^2$ which is well below the skin negative resistance mentioned above.

Finally, there is a stability requirement which limits uniform potential control over an excitable preparation to a definite area. To determine the potential distribution experimentally, a three-electrode measurement must be made. Since we could not make this measurement conveniently in our experimental chamber, we use Cole's (1968, 348) formulation for a voltage-clamped axon. This analysis is done for a circular flat membrane backed by one planar-disk current electrode and by another at a distance, δ, on its opposite side. The radius, $\bar{a}$, for the largest possible area of uniform potential distribution is

$$\bar{a} = 3.83 \Big/ \sqrt{r_2(g_3 - g_1)/\delta}$$

where g_1 (mho/cm^2) is the distal current electrode conductance, g_3 (mho/cm^2) is the absolute magnitude of the membrane negative conductance, and r_2 ($\Omega \cdot$cm) is the resistivity of the solution between the membrane and the distal current electrode. Since our arrangement (Fig. 1) of skin disk and planar-spiral current electrodes is different from the analyzed configuration, the expression for $\bar{a}$ may not be accurate for our experiments. Nevertheless, we use it as the best guide available. To compute $\bar{a}$, we assume a uniform current distribution from the current electrodes to the skin surfaces. Then the solution resistance ($128\ \Omega \cdot cm^2$) between each current electrode and the skin can be lumped together with each electrode resistance ($7\ \Omega \cdot cm^2$) to give g_1 (3.7×10^{-3} mho/cm^2). r_2 ($64\ \Omega \cdot$cm) then represents the resistivity of the path from one skin surface to the excitable membrane on the opposite skin surface. δ becomes the skin thickness which is about 0.1 mm and g_3 is the reciprocal of the lowest measured negative resistance ($150\ \Omega \cdot cm^2$). Using these values, which were chosen to give a conservative estimate of the maximum radius, $\bar{a}$ is 0.89 cm, whereas the actual disk of skin exposed to experimental solution had a radius of 0.56 cm.

RESULTS

Correlation of Current-Clamp and Voltage-Clamp Data

A few qualitative observations may be made by comparing the current-clamp data with voltage-clamp data from the same skin. Fig. 2 shows these data for three different skins. Fig. 2 *A* is an inexcitable skin characterized by its slight overshoot potential response. This response was shown by 25 out of 205 skins. The current responses for this skin under voltage clamp increase monotonically with increasing voltage-clamp steps. The skin in Fig. 2 *B* is also inexcitable but the overshoot responses (41 of 205 skins) are of a different character than those of Fig. 2 *A*. The voltage-clamp data show a noticeable clustering of the current responses indicating a prominent nonlinearity 2.5 msec after steps above 200 mv. Finally, in Fig. 2 *C*, we have an excitable skin (141 of 205 skins) with characteristic all-or-none spikes.

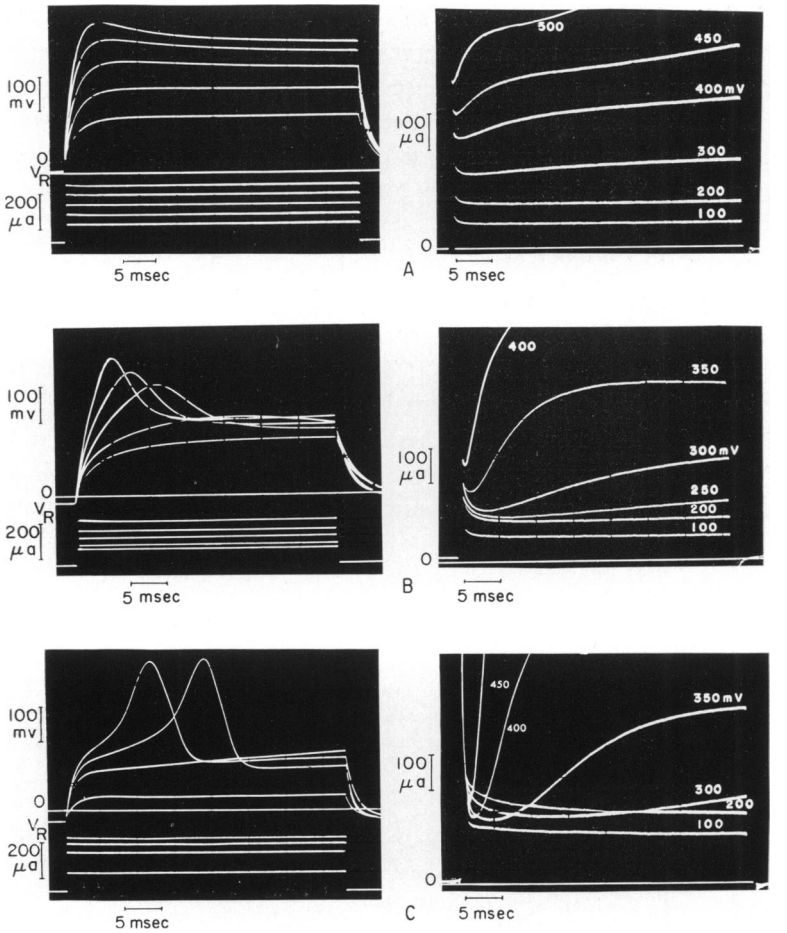

FIGURE 2 Comparison of current-clamp data (left) and voltage-clamp data (right) in three frog skins. (*A*) An inexcitable skin (slight overshoot response). (*B*) An inexcitable skin (large overshoot responses). (*C*) An excitable skin (all-or-none spike responses). In the current-clamp data, V_r denotes the resting potential difference across the skin (outside surface negative). The rectangular-current pulses result in current flow from the outside skin surface inward so that the resting skin potential polarity is reversed. The time interval between successively increasing current pulses is 30 sec. In the voltage-clamp data, the voltage step for each current response appears at the right in millivolts. The clamp system holds the skin at zero potential in the quiescent state; then the voltage steps make the outside skin surface positive with respect to the inside surface. This is also the case for voltage-clamp data in subsequent figures in which these steps are called "positive."

The significant difference between the voltage-clamp data of Fig. 2 *C* and Fig. 2 *A* or 2 *B* is the crossing of current response curves for steps above 200 mv. The transitory dipping of the current curves below previous step responses for increasing steps is indicative of a negative slope current-potential relation during the time interval in which the crossing occurs. The outstanding single observation of these experiments

(205 skins) has been that whenever spike generation occurred, it was accompanied by a crossing of current response curves in the voltage-clamp data. In cases where the above-threshold potential response was ambiguous (i.e. it was neither clearly all-or-none nor overshoot) the voltage-clamp data above 200 mv gave either a slight crossing of the current response curves or responses which were contiguous during a portion of their time course.

Electrical Parameters

Previous impedance measurements in frog skin (Cole, 1932; Teorell, 1946; Brown and Kastella, 1965) have been interpreted in terms of the incremental (dV/dI) equivalent circuit shown in Fig. 3 *A*. The resistance R'_s corresponds to nebulous conducting paths in the skin which are in series with the lumped parallel resistance-capacitance of cell membranes. The terminals of this circuit correspond to the location of the potential sensing electrodes (at the outside and inside skin surfaces) in the clamp system. If this circuit is assumed to be passive, linear, and time-invariant,

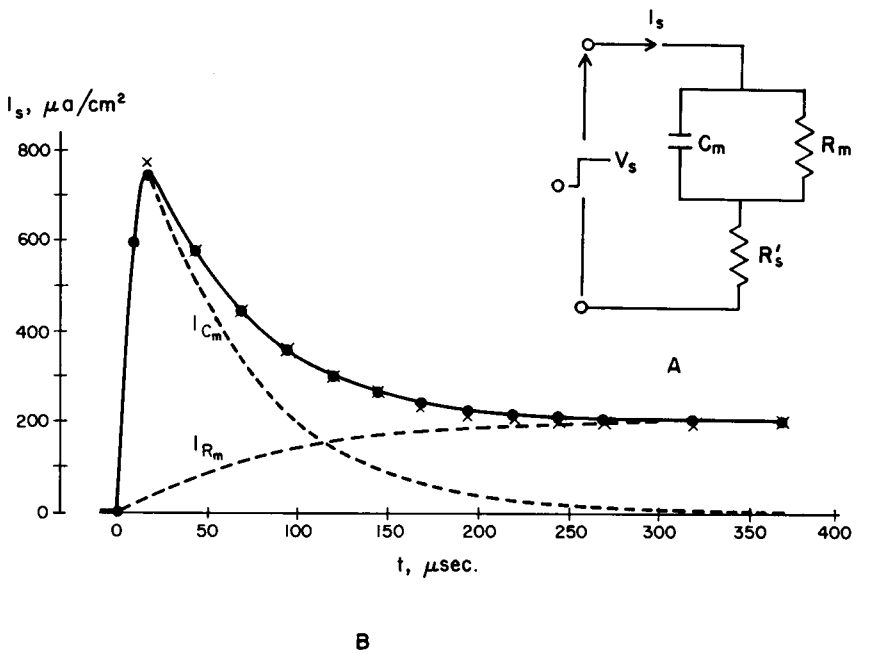

FIGURE 3 (*A*) Linear, time-invariant, equivalent circuit for the frog skin (subthreshold behavior) based upon previous impedance measurements. (*B*) The *X*'s are points on a decaying exponential curve which is the current response, I_s, of the circuit in (*A*) to an applied step voltage, V_s. The filled circles are points on the actual current response of frog skin for a positive subthreshold voltage-clamp step of 50 mv. The capacitive current, I_{Cm}, is not over and the ionic current, I_{Rm}, does not reach steady state until 300 μsec after the application of the step. This is the time required to achieve a voltage clamp of the element R_m.

the current through the circuit in response to an applied step of potential from a voltage source (Fig. 3 *B*) is

$$i_s(t) = \frac{V_s}{R'_s + R_m}\left[1 + \frac{R_m}{R'_s}\exp(-t/\tau)\right],$$

where

$$\tau = \frac{R'_s R_m}{R'_s + R_m} C_m.$$

Intuitively, for the first instant after the step, a current V_s/R'_s flows through R'_s into the capacitor supplying it with charge which raises its potential. As the capacitor becomes charged toward the potential $[R_m/(R'_s + R_m)]V_s$, its current i_{C_m} decreases while the current flow i_{R_m} through the path R'_s and R_m increases. Eventually the current flow in the circuit is through R'_s and R_m, and is given by $V_s/(R'_s + R_m)$. Note that the parameters R'_s and R_m can be obtained from the initial V_s/R'_s and long term $V_s/(R'_s + R_m)$ current values in response to the step. The time constant τ, from which C_m can be determined, is obtained from the current response curve (decay of current through the capacitor).

Fig. 3 *B* shows the skin response for a subthreshold 50 mv step change in skin potential. The response resembles that based upon the equivalent circuit and compares very well with the superposed exponential decay. The computed values of R'_s and R_m for this skin are 58 $\Omega \cdot cm^2$ and 192 $\Omega \cdot cm^2$. The time constant τ associated with the decay is 60 μsec. In ten other skins R'_s ranged from 40–80 $\Omega \cdot cm^2$; R_m, 150–1250 $\Omega \cdot cm^2$; τ, 50–120 μsec; and C_m, 1.3–5 $\mu F/cm^2$. In split skins, R'_s and the other parameters were not significantly different from intact skins. Note that the capacitive transient, which obscures direct observation of the ionic current shortly after the step is applied, cannot be reduced to less than the time constant $(R'_s R_m/R'_s + R_m)C_m$ (neglecting the source resistance of the clamp system output, which includes the current electrode resistances and the solution resistances up to the potential sensing electrodes). The capacitance C_m thus charges as though driven from a source resistance of R_m in parallel with R'_s. Unfortunately, the value of R'_s for the skin is sizeable (about 50 $\Omega \cdot cm^2$). Consequently, although the system clamps the potential difference across the skin (between the terminals of the circuit of Fig. 3 *A*) rapidly (10 μsec), the potential across the parallel combination or R_m and C_m is not clamped until 300 μsec after the subthreshold step (Fig. 3 *B*). It is at this time after the subthreshold step that the capacitor's voltage is constant and the ionic current through R_m reaches steady state. An early observation (10–300 μsec) of ionic current under voltage clamp in frog skin is therefore hindered by the long (300 μsec) capacitive transient due to the large skin R'_s, and by the fact that the excitable membrane, as represented by R_m, is not potential clamped during this capacitive transient.

Composite Step Voltage-Clamp Data

A detailed picture of the voltage-clamp data for an excitable skin (intact) is presented in Fig. 4. (Split skin gives similar data.) Part *A* of the figure shows the early character of the current responses after the applied steps (1.6 msec duration). Part *B* shows the data for long-term (42 msec duration) clamp steps. To display the time development of the negative slope, a family of I-V curves was obtained from the clamp data of Fig. 4. For a particular time after each step, the skin current I_s was plotted vs. the clamped-skin potential V_s. Fig. 5 shows these isochronal I-V curves

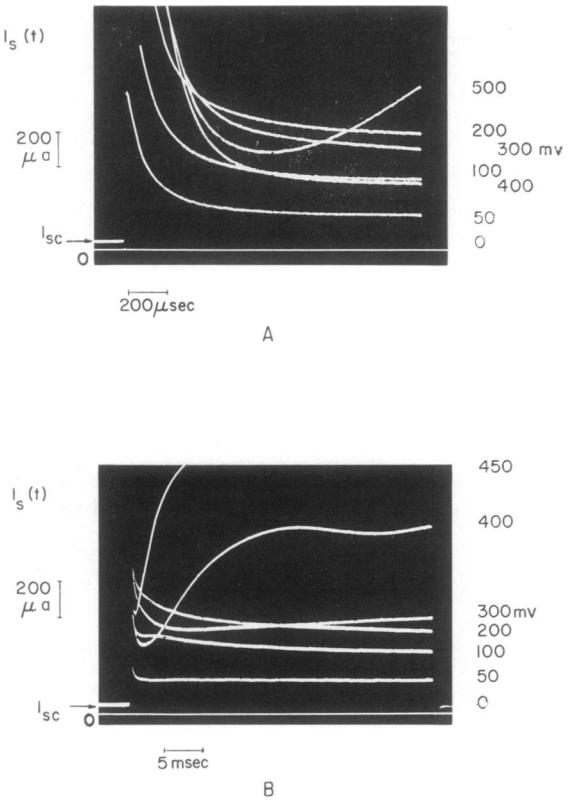

FIGURE 4 A composite set of current response curves for successive positive voltage-clamp steps across the same skin. (*A*) Short term (1.7 msec duration) clamp steps. (*B*) long term (42 msec duration) clamp steps. The time interval between successive clamp steps in both *A* and *B* is 15 sec. The magnitude of each clamp step appears at the right in millivolts. I_{sc} is the skin short-circuit current obtained when the skin potential is clamped at zero in the quiescent state.

For negative polarity clamp steps the current responses are similar but of opposite polarity, i.e., transepithelial current is directed from the inside toward the outside surface. However, the crossing of the curves occurs much less frequently corresponding to the observation that negative polarity spikes in frog skin under current clamp occur less often than positive spikes (Finkelstein, 1964).

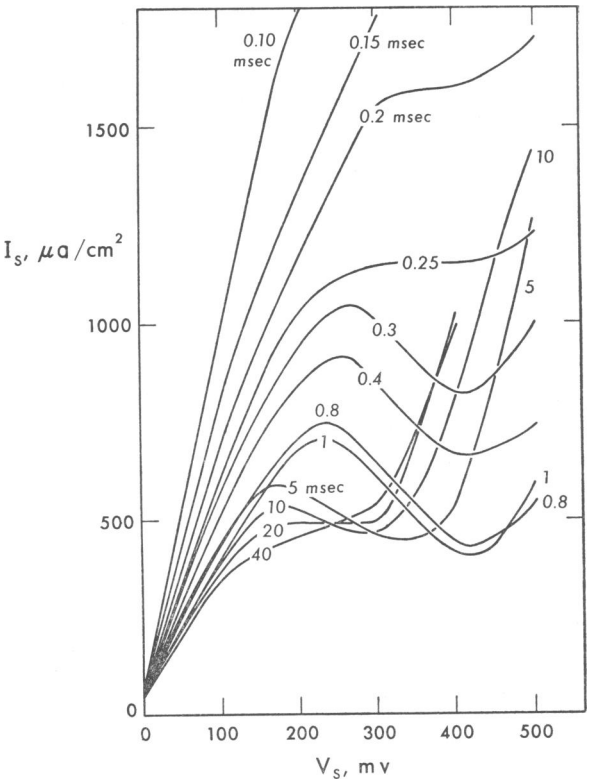

FIGURE 5 Isochronal I-V curves. These curves are produced from the voltage-clamp data of Fig. 4. The current value is plotted vs. each voltage-clamp step at constant time after the application of the clamp steps. Each curve is constructed from 10 data points.

with time as a parameter. Fig. 6 is a plot of the maximum negative resistance as represented by the reciprocal of the negative slope of the isochronal curves with time. The negative resistance apparently develops about 250 μsec after an above threshold step (> 200 mv), reaches a "quasi-steady state" rapidly (0.4 – 1.5 msec), moves slowly from this state for about 10 msec, and then disappears in the next 10 msec. Variation in the onset of the negative resistance process in 10 skins ranged from 100–360 μsec (mean ± SE = 256 ± 26 μsec). The quasi-negative resistance in 6 skins ranged from −150 to −430 Ω·cm² (mean ± SE = 289 ± 46 Ω·cm²).

The isochronal I-V curves in Fig. 5 for 100, 150, and 200 μsec are in error since the capacitive component of current was not subtracted from the clamp data for these times. In addition, as mentioned previously, the excitable membrane is not clamped in this time interval. Furthermore, although the isochronal curves are a convenient way of presenting voltage-clamp data, they are merely an expression of these data collected arbitrarily (at constant time) after a succession of different potential steps. It is important, therefore, to realize that even though these curves

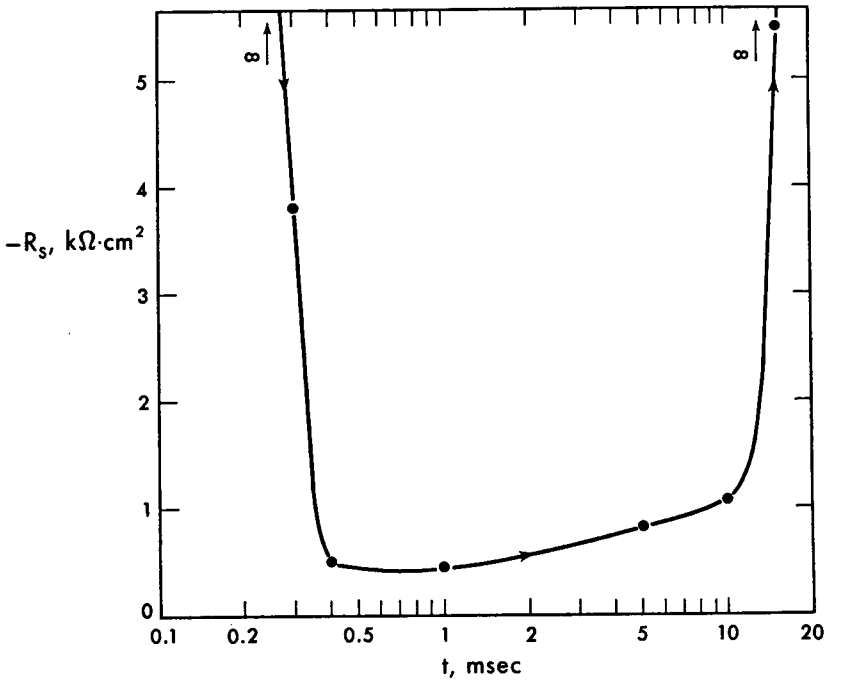

FIGURE 6 The time development of negative resistance under voltage-clamp conditions. The negative resistance at each time is obtained from the reciprocal of the maximum negative slope of the isochronal I-V curves of Fig. 5.

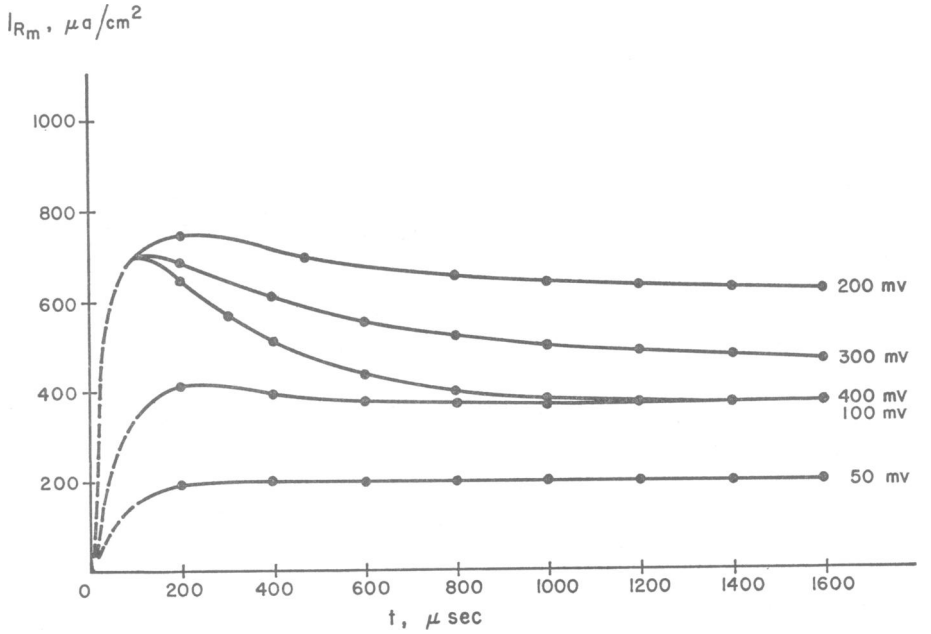

FIGURE 7 The early ionic current responses for successively increasing voltage-clamp steps (the quiescent DC current at zero clamp has been removed). The capacitive transient has been removed by the procedure described in the text. The dashed lines indicate uncertainty in this procedure. The step values refer to the change in potential across the entire skin.

show the development of a quasi-steady state negative resistance, it would be coincidental if this negative resistance and the negative resistance during current clamp excitation were the same.

Another set of voltage-clamp curves were corrected for the capacitive transient assuming that it remains constant with changes in skin potential (Teorell, 1949). The capacitance was determined from a subthreshold step as described previously. The ionic current curves are presented in Fig. 7. Although there is uncertainty in the graphical procedure for removing the capacitive transient up to 50 μsec after the step, the essential features of the isochronal I-V curves of Fig. 5 remain unchanged.

Compensated Feedback

Voltage clamp experiments were also performed using the compensated feedback scheme described by Hodgkin, Huxley, and Katz (1952). The use of an additional feedback loop in the voltage-clamp system allows reduction of R'_s (Fig. 3 *A*) to zero. Thus the early ionic current can be observed since the capacitive transient and time required to clamp the skin are also reduced when R'_s is eliminated. However, with the added compensated-feedback loop, system stability problems can occur from overcompensation for R'_s. Therefore, the magnitude of R'_s was determined from a subthreshold step measurement (uncompensated) and this parameter was used in the compensation scheme. The capacitive transient and clamping speed were thus reduced to 50 μsec with compensated feedback. The ionic current responses resembled those obtained graphically (Fig. 7) except for the superposed initial capacitive spikes which were over after the first 50 μsec.

DISCUSSION

Spike generation in frog skin under current-clamp conditions was interpreted by Finkelstein (1964) to be the result of a threshold time-variation in the resistance state of the skin. We have found under step voltage clamp that frog skin has an N-shaped I-V characteristic only if all-or-none voltage transitions can be ellicited under current clamp. A time-varying resistance may display voltage instability but only under a very specific circumstance, viz., the steady-state I-V relation characterizing the resistance must have a negative slope. Our results thus suggest that excitability in frog skin is the manifestation of a very specific type of time-varying resistance i.e., a negative resistance.

A strict definition of the term "negative resistance" requires that the stationary (V/I) and incremental (dV/dI) relation between current and potential be negative in the steady state, i.e., the relation between current and potential must have only a negative slope and can only exist in the second or fourth quadrant of the I-V plane. Usually electrical devices and excitable biological preparations do not possess this characteristic. More commonly, there exists a limited negative-slope region in

the first or third quadrant of the I-V plane. Although the stationary relation between current and potential in these quadrants is always positive, the slope may be negative. The device, when biased to operate in the negative-slope region of the I-V plane, is characterized by a negative "incremental" resistance. For most purposes, the kinetic behavior is of primary interest and the term "incremental" is assumed.

The isochronal I-V data of Fig. 5 and the negative-resistance development curve of Fig. 6 show that a quasi-steady state first quadrant negative slope occurs in frog skin.[3] Thus the range of phenomena associated with negative-resistance devices is to be expected. For example, under current-clamp sufficient current must be passed through the skin to bias it to a point (Fig. 5, 1 msec curve) between the subthreshold positive-incremental resistance region and the negative resistance region. This point corresponds to current threshold. Furthermore, the spikes on frog skin range from 200–400 mv. These large spikes occur because the negative resistance makes use of the biasing source of energy which, in the case of the skin, is the threshold current passed through it. In the resting state, nerve and muscle are already biased close to the threshold point by the ionic concentration gradients which exist, and it is the energy derived from these gradients which yields the spike.

The early clamp data indicate that the negative resistance develops after the application of a threshold skin potential. It would therefore appear that the excitable process develops in response to a sufficiently intense stimulus and that at rest the skin does not have a negative resistance. Since the negative resistance under voltage clamp only exists for 20 msec subsequent to applied step changes in skin potential, it also appears that a process occurs during excitation which results in the temporary loss of the skin's negative-resistance property. The time that the skin remains without this characteristic would thus correspond to the absolute refractory period. Notice that in the curves of Fig. 5, the low incremental resistance which exists at high skin potentials appears to move in on the negative-resistance region which eventually disappears with time. Further characterization of the N-shaped I-V relation in frog skin and its dependence on specific ions will appear in a subsequent paper.

We wish to express our appreciation to Dr. Kenneth S. Cole for many enlightening discussions and his helpful comments on the manuscript.

This work was partially supported by National Institutes of Health Grant (5-T1 GM 829 06), by AEC contract AT(11-1)-34 project 136-8, and by NSF GB 1928.

Received for publication 25 June 1968 and revised form 17 October 1968.

REFERENCES

BROWN, A. C., and K. G. KASTELLA. 1965. *Biophys. J.* **5**:591.
COLE, K. S. 1932. *J. Gen. Physiol.* **15**:641.

[3] A third quadrant negative slope also was found but it occurred less often.

COLE, K. S. 1968. Membranes, Ions, and Impulses. University of California Press, Berkeley, Calif.
COLE, K. S., and U. KISHIMOTO. 1962. *Science.* **136:**381.
COLE, K. S., and J. W. MOORE. 1960. *J. Gen. Physiol.* **44:**123.
FINKELSTEIN, A. 1961. *Nature.* **190:**1119.
FINKELSTEIN, A. 1964. *J. Gen. Physiol.* **47:**545.
FISHMAN, H. M., and R. I. MACEY. 1968. *Biochim. Biophys. Acta.* **150:**482.
HODGKIN, A. L., A. F. HUXLEY, and B. KATZ. 1952. *J. Physiol.* (*London*). **116:**424.
LINDEMANN, B. 1965. *Biol. Bull.* **129:**391.
LINDEMANN, B., and U. THORNS. 1967. *Science.* **158:**1473.
TEORELL, T. 1946. *Acta Physiol. Scand.* **12:**235.
TEORELL, T. 1949. *Arch. Sci. Physiol.* **3:**205.
USSING, H. H., and K. ZERAHN. 1951. *Acta Physiol. Scand.* **23:**110.